

# Proton Structure from the Measurement of 2S-2P Transition Frequencies of Muonic Hydrogen

Aldo Antognini,<sup>1,2\*</sup> François Nez,<sup>3</sup> Karsten Schuhmann,<sup>2,4</sup> Fernando D. Amaro,<sup>5</sup> François Biraben,<sup>3</sup> João M. R. Cardoso,<sup>5</sup> Daniel S. Covita,<sup>5,6</sup> Andreas Dax,<sup>7</sup> Satish Dhawan,<sup>7</sup> Marc Diepold,<sup>1</sup> Luis M. P. Fernandes,<sup>5</sup> Adolf Giesen,<sup>4,8</sup> Andrea L. Gouvea,<sup>5</sup> Thomas Graf,<sup>8</sup> Theodor W. Hänsch,<sup>1,9</sup> Paul Indelicato,<sup>3</sup> Lucile Julien,<sup>3</sup> Cheng-Yang Kao,<sup>10</sup> Paul Knowles,<sup>11</sup> Franz Kottmann,<sup>2</sup> Eric-Olivier Le Bigot,<sup>3</sup> Yi-Wei Liu,<sup>10</sup> José A. M. Lopes,<sup>5</sup> Livia Ludhova,<sup>11</sup> Cristina M. B. Monteiro,<sup>5</sup> François Mulhauser,<sup>11</sup> Tobias Nebel,<sup>1</sup> Paul Rabinowitz,<sup>12</sup> Joaquim M. F. dos Santos,<sup>5</sup> Lukas A. Schaller,<sup>11</sup> Catherine Schwob,<sup>3</sup> David Taqqu,<sup>13</sup> João F. C. A. Veloso,<sup>6</sup> Jan Vogelsang,<sup>1</sup> Randolph Pohl<sup>1</sup>

Accurate knowledge of the charge and Zemach radii of the proton is essential, not only for understanding its structure but also as input for tests of bound-state quantum electrodynamics and its predictions for the energy levels of hydrogen. These radii may be extracted from the laser spectroscopy of muonic hydrogen ( $\mu\text{p}$ , that is, a proton orbited by a muon). We measured the  $2S_{1/2}^{F=0} - 2P_{3/2}^{F=1}$  transition frequency in  $\mu\text{p}$  to be 54611.16(1.05) gigahertz (numbers in parentheses indicate one standard deviation of uncertainty) and reevaluated the  $2S_{1/2}^{F=1} - 2P_{3/2}^{F=2}$  transition frequency, yielding 49881.35(65) gigahertz. From the measurements, we determined the Zemach radius,  $r_Z = 1.082(37)$  femtometers, and the magnetic radius,  $r_M = 0.87(6)$  femtometer, of the proton. We also extracted the charge radius,  $r_E = 0.84087(39)$  femtometer, with an order of magnitude more precision than the 2010-CODATA value and at  $7\sigma$  variance with respect to it, thus reinforcing the proton radius puzzle.

As the simplest of all stable atoms, hydrogen (H) is unique in its use for comparison between theory and experiment of bound-state energy level structures. Observation of the simple Balmer series in the H emission spectrum inspired the Bohr atomic model and quantum mechanics. More precise measurements of the first Balmer line revealed a splitting of the  $n = 2$  states ( $n$  is the principal quantum number) arising from the electron's magnetic moment (spin-orbit interaction). Such data represented the crucial validation of the Dirac equation. However, further direct investigation of the hydrogen  $2S_{1/2} - 2P_{1/2}$  energy splitting (Lamb shift) and the  $1S$  hyperfine splitting (HFS) in 1947 by means of microwave spec-

troscopy revealed a small deviation from the prediction of the Dirac equation. This fueled the development of quantum electrodynamics (QED). Precision measurements of H transition frequencies have been pursued in the past 40 years by laser spectroscopy. In spite of the considerable advances in both experimental (spectroscopy) and theoretical (bound-state QED) accuracy, the comparison between theory and experiment has been hampered by the lack of accurate knowledge of the proton charge and magnetization distributions. The proton structure is important because an electron in an S state has a nonzero probability to be inside the proton. The attractive force between the proton and the electron is thereby reduced because the electric field inside the charge distribution is smaller than the corresponding field produced by a point charge. Thus, the measured transition frequencies depend on the proton size.

Although the shifts of the energy levels associated with the proton finite size are small, it is the 1 to 2% relative uncertainty of the proton charge radius,  $r_E$  (1–3), and Zemach radius,  $r_Z$  (4, 5), respectively, that presently limit the theoretical predictions of the Lamb shift and the HFS in H. The Zemach radius reflects the spatial distribution of magnetic moments smeared out (convoluted) by the charge distribution of the proton.

Historically, these radii were derived from measurements of the differential cross section in elastic electron-proton scattering. An independent and more precise determination of these radii can be achieved by laser spectroscopy of the exotic

“muonic hydrogen” atom,  $\mu\text{p}$  (6). Such atoms are formed by a proton and a negative muon,  $\mu^-$ , a particle whose mass,  $m_\mu$ , is 207 times that of the electron,  $m_e$ . Its atomic energy levels are affected by the finite size of the proton charge distribution (neglecting higher moments of the charge distribution and higher orders in  $\alpha$ ) by

$$\Delta E_{\text{finite size}} = \frac{2\pi Z\alpha}{3} r_E^2 |\Psi(0)|^2 \quad (1)$$

where  $\Psi(0)$  is the atomic wave function at the origin,  $\alpha$  the fine structure constant, and  $Z = 1$  the proton charge. For S states,  $|\Psi(0)|^2$  is proportional to  $m_r^3$ , with  $m_r \approx 186m_e$  being the reduced mass of the  $\mu\text{p}$  system. The muon Bohr radius is 186 times smaller than the electron Bohr radius in H, resulting in a strongly increased sensitivity of  $\mu\text{p}$  to the proton finite size.

We have recently performed the measurement of the  $2S_{1/2}^{F=1} - 2P_{3/2}^{F=2}$  transition (Fig. 1 C) in  $\mu\text{p}$ , which led to a determination of  $r_E$  with a relative accuracy  $u_r = 8 \times 10^{-4}$  (6). Yet the  $r_E$  value obtained is seven standard deviations smaller than the world average (7) based on H spectroscopy and elastic electron scattering. This discrepancy has triggered a lively discussion addressing the accuracy of these experiments, bound-state QED, the proton structure, the Rydberg constant ( $R_\infty$ ), and possibilities of new physics.

**Principle and measurements.** The principle of the muonic hydrogen Lamb shift experiment is to form muonic hydrogen in the 2S state (Fig. 1A) and then measure the 2S-2P energy splitting (Fig. 1C) by means of laser spectroscopy (Fig. 1B) using the setup sketched in Fig. 2 (6).

Negative muons from the proton accelerator of the Paul Scherrer Institute, Switzerland, are stopped in  $\text{H}_2$  gas at 1 hPa and 20°C, where highly excited  $\mu\text{p}$  atoms ( $n \approx 14$ ) are formed. Most of these deexcite quickly to the 1S ground state (8), but  $\sim 1\%$  populate the long-lived 2S state (Fig. 1A), whose lifetime is  $\sim 1 \mu\text{s}$  at 1 hPa (9). A 5-ns laser pulse with a wavelength tunable from 5.5 to 6  $\mu\text{m}$  (10, 11) illuminates the target gas volume, about 0.9  $\mu\text{s}$  after the muon reached the target. On-resonance light induces  $2S \rightarrow 2P$  transitions, which are immediately followed by  $2P \rightarrow 1S$  deexcitation via 1.9-keV  $K_\alpha$  x-ray emission (lifetime  $\tau_{2P} = 8.5$  ps). A resonance curve is obtained by measuring the number of 1.9-keV x-rays in time coincidence with the laser pulse (i.e., within a time window of 0.900 to 0.975  $\mu\text{s}$  after the muon entry into the target) as a function of the laser wavelength. The 75-ns width of this window corresponds to the confinement time of the laser light within the multipass mirror cavity surrounding the gas target.

We have measured the two 2S-2P transitions depicted in Fig. 1C, one from the singlet state with frequency  $\nu_s = \nu(2S_{1/2}^{F=0} - 2P_{3/2}^{F=1})$  and wavelength  $\lambda_s \approx 5.5 \mu\text{m}$  and the other from the triplet state with  $\nu_t = \nu(2S_{1/2}^{F=1} - 2P_{3/2}^{F=2})$  and  $\lambda_t \approx 6.0 \mu\text{m}$ . For the latter, we present an updated analysis of the data presented in (6).

<sup>1</sup>Max-Planck-Institut für Quantenoptik, 85748 Garching, Germany. <sup>2</sup>Institute for Particle Physics, Eidgenössische Technische Hochschule (ETH) Zürich, 8093 Zürich, Switzerland. <sup>3</sup>Laboratoire Kastler Brossel, École Normale Supérieure, CNRS and Université Pierre et Marie Curie (UPMC), 75252 Paris, CEDEX 05, France. <sup>4</sup>Dausinger and Giesen GmbH, Rotebühlstraße 87, 70178 Stuttgart, Germany. <sup>5</sup>Departamento de Física, Universidade de Coimbra, 3004-516 Coimbra, Portugal. <sup>6</sup>IN, Departamento de Física, Universidade de Aveiro, 3810-193 Aveiro, Portugal. <sup>7</sup>Physics Department, Yale University, New Haven, CT 06520–8121, USA. <sup>8</sup>Institut für Strahlwerkzeuge, Universität Stuttgart, 70569 Stuttgart, Germany. <sup>9</sup>Ludwig-Maximilians-Universität, Munich, Germany. <sup>10</sup>Physics Department, National Tsing Hua University, Hsinchu 300, Taiwan. <sup>11</sup>Département de Physique, Université de Fribourg, 1700 Fribourg, Switzerland. <sup>12</sup>Department of Chemistry, Princeton University, Princeton, NJ 08544–1009, USA. <sup>13</sup>Paul Scherrer Institute, 5232 Villigen-PSI, Switzerland.

\*To whom correspondence should be addressed. E-mail: aldo@phys.ethz.ch

Figure 3 shows the two measured  $\mu\text{p}$  resonances. Details of the data analysis are given in (12). The laser frequency was changed every few hours, and we accumulated data for up to 13 hours per laser frequency. The laser frequency was calibrated [supplement in (6)] by using well-known water absorption lines. The resonance positions corrected for laser intensity effects using the line shape model (12) are

$$\nu_s = 54611.16(1.00)^{\text{stat}}(30)^{\text{sys}} \text{ GHz} \quad (2)$$

$$\nu_t = 49881.35(57)^{\text{stat}}(30)^{\text{sys}} \text{ GHz} \quad (3)$$

where “stat” and “sys” indicate statistical and systematic uncertainties, giving total experimental uncertainties of 1.05 and 0.65 GHz, respectively. Although extracted from the same data, the frequency value of the triplet resonance,  $\nu_t$ , is slightly more accurate than in (6) owing to several improvements in the data analysis. The fitted line widths are 20.0(3.6) and 15.9(2.4) GHz, respectively, compatible with the expected 19.0 GHz resulting from the laser bandwidth (1.75 GHz at full width at half maximum) and the Doppler broadening (1 GHz) of the 18.6-GHz natural line width.

The systematic uncertainty of each measurement is 300 MHz, given by the frequency calibration uncertainty arising from pulse-to-pulse fluctuations in the laser and from broadening effects occurring in the Raman process. Other systematic corrections we have considered are the Zeeman shift in the 5-T field (<60 MHz), AC and DC Stark shifts (<1 MHz), Doppler shift (<1 MHz), pressure shift (<2 MHz), and black-body radiation shift (<<1 MHz). All these typically important atomic spectroscopy systematics are small because of the small size of  $\mu\text{p}$ .

**The Lamb shift and the hyperfine splitting.** From these two transition measurements, we can independently deduce both the Lamb shift ( $\Delta E_L = \Delta E_{2P_{1/2}-2S_{1/2}}$ ) and the 2S-HFS splitting ( $\Delta E_{\text{HFS}}$ ) by the linear combinations (13)

$$\frac{1}{4}h\nu_s + \frac{3}{4}h\nu_t = \Delta E_L + 8.8123(2)\text{meV}$$

$$h\nu_s - h\nu_t = \Delta E_{\text{HFS}} - 3.2480(2)\text{meV} \quad (4)$$

Finite size effects are included in  $\Delta E_L$  and  $\Delta E_{\text{HFS}}$ . The numerical terms include the calculated values of the 2P fine structure, the  $2P_{3/2}$  hyperfine splitting, and the mixing of the 2P states (14–18). The finite proton size effects on the 2P fine and hyperfine structure are smaller than  $1 \times 10^{-4}$  meV because of the small overlap between the 2P wave functions and the nucleus. Thus, their uncertainties arising from the proton structure are negligible. By using the measured transition frequencies  $\nu_s$  and  $\nu_t$  in Eqs. 4, we obtain (1 meV corresponds to 241.79893 GHz)

$$\Delta E_L^{\text{exp}} = 202.3706(23) \text{ meV} \quad (5)$$

$$\Delta E_{\text{HFS}}^{\text{exp}} = 22.8089(51) \text{ meV} \quad (6)$$

The uncertainties result from quadratically adding the statistical and systematic uncertainties of  $\nu_s$  and  $\nu_t$ .

**The charge radius.** The theory (14, 16–22) relating the Lamb shift to  $r_E$  yields (13):

$$\Delta E_L^{\text{th}} = 206.0336(15) - 5.2275(10)r_E^2 + \Delta E_{\text{TPE}} \quad (7)$$

where  $E$  is in meV and  $r_E$  is the root mean square (RMS) charge radius given in fm and defined as  $r_E^2 = \int d^3r r^2 \rho_E(r)$  with  $\rho_E$  being the normalized proton charge distribution. The first term on the right side of Eq. 7 accounts for radiative, relativistic, and recoil effects. Fine and hyperfine corrections are absent here as a consequence of Eqs. 4. The other terms arise from the proton structure. The leading finite size effect  $-5.2275(10)r_E^2$  meV is approximately given by Eq. 1 with corrections given in (13, 17, 18). Two-photon exchange (TPE) effects, including the proton polarizability, are covered by the term  $\Delta E_{\text{TPE}} = 0.0332(20)$  meV (19, 24–26). Issues related with TPE are discussed in (12, 13).

The comparison of  $\Delta E_L^{\text{th}}$  (Eq. 7) with  $\Delta E_L^{\text{exp}}$  (Eq. 5) yields

$$r_E = 0.84087(26)^{\text{exp}}(29)^{\text{th}} \text{ fm} \\ = 0.84087(39) \text{ fm} \quad (8)$$

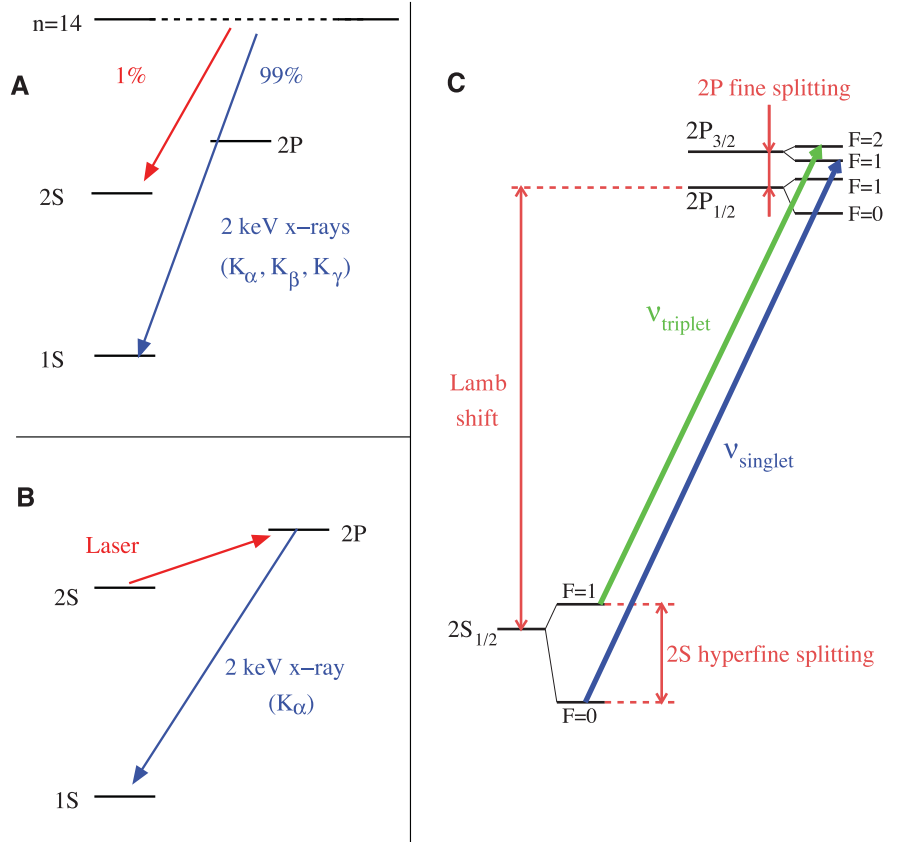


**Fig. 1.** (A) Formation of  $\mu\text{p}$  in highly excited states and subsequent cascade with emission of “prompt”  $K_{\alpha, \beta, \gamma}$ . (B) Laser excitation of the 2S-2P transition with subsequent decay to the ground state with  $K_{\alpha}$  emission. (C) 2S and 2P energy levels. The measured transitions  $\nu_s$  and  $\nu_t$  are indicated together with the Lamb shift, 2S-HFS, and 2P-fine and hyperfine splitting.

This  $r_E$  value is compatible with our previous  $\mu\text{p}$  result (6), but 1.7 times more precise, and is now independent of the theoretical prediction of the 2S-HFS. Although an order of magnitude more precise, the  $\mu\text{p}$ -derived proton radius is at  $7\sigma$  variance with the CODATA-2010 (7) value of  $r_E = 0.8775(51)$  fm based on H spectroscopy and electron-proton scattering.

**Magnetic and Zemach radii.** The theoretical prediction (17, 18, 27–29) of the 2S-HFS is (13)

$$\Delta E_{\text{HFS}}^{\text{th}} = 22.9763(15) - 0.1621(10)r_Z + \Delta E_{\text{HFS}}^{\text{pol}} \quad (9)$$

where  $E$  is in meV and  $r_Z$  is in fm. The first term is the Fermi energy arising from the interaction between the muon and the proton magnetic moments, corrected for radiative and recoil contributions, and includes a small dependence of  $-0.0022r_E^2$  meV =  $-0.0016$  meV on the charge radius (13).

The leading proton structure term depends on  $r_Z$ , defined as

$$r_Z = \int d^3r \int d^3r' r' \rho_E(r) \rho_M(\mathbf{r} - \mathbf{r}') \quad (10)$$

with  $\rho_M$  being the normalized proton magnetic moment distribution. The HFS polariz-





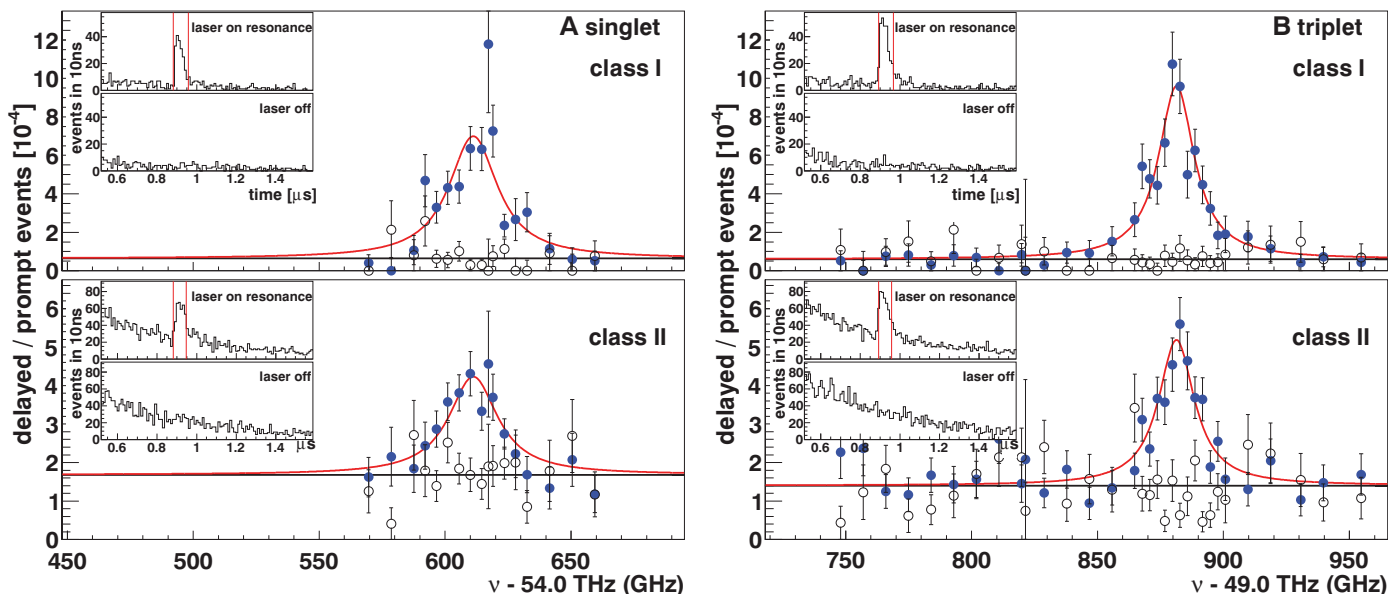


**Fig. 3.** Muonic hydrogen resonances (solid circles) for singlet  $\nu_s$  (A) and triplet  $\nu_t$  (B) transitions. Open circles show data recorded without laser pulses. Two resonance curves are given for each transition to account for two different classes, I and II, of muon decay electrons (12). Error bars indicate the standard error. (Insets) The time spectra of  $K_{\alpha}$  x-rays. The vertical lines indicate the laser time window.

and the “pure” 2S-2P Lamb shift. By comparison with theoretical predictions, two proton-structure parameters are determined:  $r_E = 0.84087(39)$  fm and  $r_Z = 1.082(37)$  fm. These radii play a crucial role in the understanding of the atomic hydrogen spectrum (bound-state QED). They also provide information needed to test quantum chromodynamics in the nonperturbative region.

Subtracting the H(1S) and H(2S) Lamb shifts, computed by using the muonic  $r_E$ , from the measured 1S–2S transition frequency in H gives  $R_{\infty} = 3.2898419602495(10)(25) \times 10^{15}$  Hz/c. The first uncertainty of 1.0 kHz/c and the second of 2.5 kHz/c originate from the uncertainties of the muonic  $r_E$  and QED theory in H, respectively. This  $R_{\infty}$  deviates by  $-115$  kHz/c, corresponding to 6.6 standard deviations, from the CODATA (7) value but is six times more precise (relative accuracy of  $u_r = 8 \times 10^{-13}$ ).

Our value of the proton charge radius  $r_E(p)$  can be used to determine a new deuteron charge radius,  $r_E(d)$ , by using the accurately measured isotope shift of the 1S–2S transition in H and D (48). From equation 4 of (48)

$$r_E^2(d) - r_E^2(p) = 3.82007(65) \text{ fm}^2 \quad (12)$$

we obtain a precise value of the deuteron RMS charge radius

$$r_E(d) = 2.12771(22) \text{ fm} \quad (13)$$

in agreement with  $r_E(d) = 2.130(10)$  fm (49) from electron-deuteron scattering but more than an order of magnitude more precise. The CODATA (7) value  $r_E(d) = 2.1424(25)$  fm is in disagreement, because it is dominantly based on the  $7\sigma$  discrepant  $r_E(p)$  value of CODATA combined with Eq. 12. The Lamb shift in muonic deuterium  $\mu d$  can provide an independent  $r_E(d)$  value.

#### References and Notes

- J. C. Bernauer *et al.*, *Phys. Rev. Lett.* **105**, 242001 (2010).
- X. Zhan *et al.*, *Phys. Lett. B* **705**, 59 (2011).
- P. G. Blunden, I. Sick, *Phys. Rev. C Nucl. Phys.* **72**, 057601 (2005).
- J. Friar, I. Sick, *Phys. Lett. B* **579**, 285 (2004).
- M. O. Distler, J. C. Bernauer, T. Walcher, *Phys. Lett. B* **696**, 343 (2011).
- R. Pohl *et al.*, *Nature* **466**, 213 (2010).
- P. J. Mohr, B. N. Taylor, D. B. Newell, *Rev. Mod. Phys.* **84**, 1527 (2012).
- R. Pohl, *Hyperfine Interact.* **193**, 115 (2009).
- R. Pohl *et al.*, *Phys. Rev. Lett.* **97**, 193402 (2006).
- A. Antognini *et al.*, *IEEE J. Quantum Electron.* **45**, 993 (2009).
- A. Antognini *et al.*, *Opt. Commun.* **253**, 362 (2005).
- Materials and methods are available as supplementary materials on Science Online.
- A. Antognini *et al.*, *Ann. Phys.*, published online 31 December 2012 (10.1016/j.aop.2012.12.003).
- K. Pachucki, *Phys. Rev. A* **53**, 2092 (1996).
- A. P. Martynenko, *Phys. Atomic Nuclei* **71**, 125 (2008).
- U. D. Jentschura, *Ann. Phys.* **326**, 500 (2011).
- E. Borie, *Ann. Phys.* **327**, 733 (2012).
- E. Borie, <http://arxiv.org/abs/1103.1772v6> (2012).
- K. Pachucki, *Phys. Rev. A* **60**, 3593 (1999).
- M. I. Eides, H. Grotch, V. A. Shelyuto, *Phys. Rep.* **342**, 63 (2001).
- S. G. Karshenboim, E. Y. Korzinnin, V. G. Ivanov, V. A. Shelyuto, *JETP Lett.* **92**, 8 (2010).
- S. G. Karshenboim, V. G. Ivanov, E. Y. Korzinnin, *Phys. Rev. A* **85**, 032509 (2012).
- U. D. Jentschura, *Phys. Rev. A* **84**, 012505 (2011).
- C. E. Carlson, M. Vanderhaeghen, *Phys. Rev. A* **84**, 020102 (2011).
- M. C. Birse, J. A. McGovern, *Eur. Phys. J. A* **48**, 120 (2012).
- R. J. Hill, G. Paz, *Phys. Rev. Lett.* **107**, 160402 (2011).
- A. P. Martynenko, *Phys. Rev. A* **71**, 022506 (2005).
- C. E. Carlson, V. Nazaryan, K. Griffioen, *Phys. Rev. A* **83**, 042509 (2011).
- E. Cherednikova, R. Faustov, A. Martynenko, *Nucl. Phys. A* **703**, 365 (2002).
- A. V. Volotka, V. M. Shabaev, G. Plunien, G. Soff, *Eur. Phys. J. D* **33**, 23 (2005).
- A. Dupays, A. Beswick, B. Lepetit, C. Rizzo, D. Bakalov, *Phys. Rev. A* **68**, 052503 (2003).
- J. C. Bernauer *et al.*, *Phys. Rev. Lett.* **107**, 119102 (2011).
- I. T. Lorenz, H.-W. Hammer, U. Meißner, *Eur. Phys. J. A* **48**, 151 (2012).
- R. Pohl, R. Gilman, G. A. Miller, K. Pachucki, <http://arxiv.org/abs/1301.0905> (2013).

- U. D. Jentschura, *Eur. Phys. J. D* **61**, 7 (2011).
- J. D. Carroll, A. W. Thomas, J. Rafelski, G. A. Miller, <http://arxiv.org/abs/1108.2541v1> (2011).
- A. De Rijula, *Phys. Lett. B* **697**, 26 (2011).
- J. L. Friar, I. Sick, *Phys. Rev. A* **72**, 040502 (2005).
- I. C. Cloët, G. A. Miller, *Phys. Rev. C Nucl. Phys.* **83**, 012201(R) (2011).
- A. Pineda, *Phys. Rev. C Nucl. Phys.* **71**, 065205 (2005).
- U. D. Jentschura, *Ann. Phys.* **326**, 516 (2011).
- J.-P. Karr, L. Hilico, *Phys. Rev. Lett.* **109**, 103401 (2012).
- G. A. Miller, A. W. Thomas, J. D. Carroll, J. Rafelski, *Phys. Rev. A* **84**, 020101(R) (2011).
- C. G. Parthey *et al.*, *Phys. Rev. Lett.* **107**, 203001 (2011).
- R. J. Hill, G. Paz, *Phys. Rev. D* **82**, 113005 (2010).
- C. E. Carlson, B. C. Millow, *Phys. Rev. D* **86**, 035013 (2012).
- B. Batell, D. McKeen, M. Pospelov, *Phys. Rev. Lett.* **107**, 011803 (2011).
- C. G. Parthey *et al.*, *Phys. Rev. Lett.* **104**, 233001 (2010).
- I. Sick, D. Trautmann, *Nucl. Phys. A* **637**, 559 (1998).

**Acknowledgments:** We thank L. M. Simons, B. Leoni, H. Brückner, K. Linner, W. Simon, J. Alpstäg, Z. Hochman, N. Schlumpf, U. Hartmann, S. Ritt, M. Gaspar, M. Horisberger, B. Weichelt, J. Früchtenicht, A. Voss, M. Lariouev, F. Dausinger, and K. Kirch for their contributions. We acknowledge support from the Max Planck Society and the Max Planck Foundation, the Swiss National Science Foundation (projects 200020-100632 and 200021-138175/1), the Swiss Academy of Engineering Sciences, the Bonus Qualité Recherche de l’Unités de Formations et de Recherche de physique fondamentale et appliquée de l’UPMC, the program PAI Germaine de Staël no. 07819NH du ministère des affaires étrangères France, the Ecole Normale Supérieure (ENS), UPMC, CNRS, and the Fundação para a Ciência e a Tecnologia (FCT, Portugal) and Fundo Europeu De Desenvolvimento Regional (project PTDC/FIS/102110/2008 and grant SFRH/BPD/46611/2008). P.I. acknowledges support by the ExtreMe Matter Institute, Helmholtz Alliance HA216/EMMI. T.N. and R.P. were in part supported by the European Research Council (ERC) Starting Grant no. 279765. A.L.G. received support from FCT through program grant SFRH/BD/66731/2009.

#### Supplementary Materials

Materials and Methods  
Supplementary Text  
References